Chapter 2
Luminescent Study of Recombination Processes in the Single-Crystal Silicon and Silicon Structures Fabricated Using High-Efficiency Solar Cell Technology

A.M. Emel'yanov

Abstract Some results of the author's researches in the last decade of the luminescence in the region of the fundamental absorption edge (edge luminescence) of the single-crystal silicon (c-Si), including structures which were made using high-efficiency solar cell technology, are summarized and systematized. This chapter presents experimental evidences and justifications of the dominant mechanism of radiative recombination in c-Si and of the dependence of the intensity of the edge luminescence on the intensity of its excitation. Considerable consideration is given to the study of recombination parameters at high excitation intensities of the edge luminescence in the structures fabricated using high-efficiency solar cell technology.

1 Introduction

Single-crystal silicon (c-Si) is a nondirect-gap semiconductor and, therefore, has been regarded as an inefficient source of luminescence during many decades. But relatively recently it was experimentally demonstrated that in c-Si it is possible to achieve the edge luminescence external quantum efficiencies (η_{ext}) which are very high in magnitude for the class of indirect-gap semiconductors (by edge luminescence it is meant luminescence in the region of the fundamental absorption edge). As far as we know, the present-day record parameter at room temperature is $\eta_{ext} = 6$ % for photoluminescence (PL) of c-Si with no p–n junction [1]. A value $\eta_{ext} = 0.6$ % [2] for electroluminescence (EL) of Si-based light-emitting diodes (LEDs) at room temperature for the first time was achieved in [2]. In the case of EL, such value of η_{ext} was obtained for p–n junctions in c-Si structures fabricated by the

A.M. Emel'yanov (✉)
Ioffe Physical-Technical Institute of the Russian Academy of Sciences,
Politekhnicheskaya 26, St. Petersburg 194021, Russia
e-mail: Emelyanov@mail.ioffe.ru; Emelyanov.49@inbox.ru

X. Wang and Z.M. Wang (eds.), *High-Efficiency Solar Cells: Physics, Materials, and Devices*, Springer Series in Materials Science 190, DOI 10.1007/978-3-319-01988-8_2,

high-efficiency solar cell technology. The large values of η_{ext} make it possible to use the edge luminescence of c-Si in Si-based optoelectronic devices. The author of this work some years ago achieved high values of the integrated edge EL power and the emissive power per unit surface area for LEDs, fabricated using high-efficiency solar cell technology. This defines one of the reasons of interest in the investigations described below.

The efficiency of the edge luminescence of c-Si depends on the effective lifetime of minority charge carriers (τ) and their diffusion length (L_D) (i.e., the parameters defining the characteristics of many semiconductor devices including solar cells). Therefore, in the last few years, a large number of studies, in which the parameters of edge luminescence of c-Si were used to determine the lifetime τ or the diffusion length L_D, the distribution of τ or L_D over the area of semiconductor wafers at different stages of device fabrication, and the dependence of τ or L_D on the concentration of minority charge carriers, have been published (see, e.g., [3–12]). The PL measurements present contactless techniques, and, according to [3], PL and EL techniques are most sensitive for determining the effective lifetimes. In addition, the authors of [3, 4] state that, in contrast to the photoconductivity measurements widely used to determine lifetimes, the quasi-steady-state luminescence technique is practically insensitive to the space charge region (SCR) in the single crystal and, in the cases of practical importance, to the capture of minority charge carriers by trapping centers. According to the description of products of the world-famous firm Hamamatsu, "detection of luminescence signals from wafer, solar cells and solar panels have become major techniques for characterization and quality inspection." Hamamatsu offers a complete "luminescence analysis system" as well as individual cameras for luminescence imaging.

In a basis of luminescent methods for determining τ and L_D lies the dependence of the radiative recombination rate in a unit volume of semiconductor (R) on the free carrier concentration. In general, this dependence is determined by the mechanism of radiative recombination. But earlier in opinion of the author there were no convincing experimental proofs of the mechanism of radiative recombination in c-Si at room temperature. Such views were based on theoretical estimates. In accordance with them at room temperature dominate or the radiative recombination of free charge carriers (see for example [13]), or approximately equal the contributions of the radiative recombination of free charge carriers and free excitons (see for example the review of the literature in [15]). Usually the dependence of the radiative recombination rate R on the concentrations of free electrons (n) and holes (p) is described by the formula

$$R = Bnp, \tag{2.1}$$

where B—radiative recombination coefficient. At a relatively small n and p, B not depend on n and p (see for example [13]). But with the growth of n and/or p, according to the calculations of some researchers, it may vary. This change at the various mechanisms of the radiative recombination can be due to various reasons and therefore be described by various dependences. For example, the authors of work [13] associated decrease of B with screening of Coulomb interaction among

the free carriers. At the exciton mechanism of radiative recombination the value R is determined by the formula

$$R = n_{ex}/\tau_{ex}, \tag{2.2}$$

where τ_{ex}—radiative lifetime of excitons and n_{ex}—concentration of free excitons. According to the results of [14], n_{ex} may depend on the concentration of free charge carriers due to screening of Coulomb interaction among charge carriers in excitons. This effect can also influence the value of B. Proved by the author of the present work in recent years the representations of the dominant mechanism of radiative recombination via free excitons in c-Si in a wide range of temperatures (including room temperatures) are the second reason of interest in the investigations presented below.

The distinguishing features of present work from similar works of other researchers are using a significantly higher intensity of luminescence excitation, especially manufacturing structures and in some cases combined impact on the structure of the two sources of luminescence excitation. For example it was shown that the linear or close-to-linear portions of the dependences of the edge luminescence intensity of c-Si on the luminescence excitation intensity under high injection levels are caused by the existence of linear or close-to-linear portions of the dependences of the free exciton concentration on the free carrier concentration at sufficiently high free carrier concentrations. Under these conditions the value of R cannot be described by formula (2.1). This is the third major reason of interest to the research results shown below.

In this work the results of the works first published in [15–22, 34] by publisher «Pleiades Publishing, Inc.» http://www.maikonline.com, http://www.maik.ru are summarized and combined.

2 Experimental Details

For the measurement of the EL and PL spectra, the light emitted from a surface of sample was focused by a system of lenses onto the entrance slit of a monochromator and detected at the exit with an uncooled InGaAs diode. The spectra were corrected for the spectral characteristic of the photodetector and the entire optical tract. The EL and PL kinetics was measured using a Ge or a Si photodetector operating at room temperature, which provided a time constant of ~1 μs in response to a rectangular pulse of light. The EL was excited by voltage pulses with a repetition frequency about 30 Hz applied to the c-Si diode. The pulses had a rectangular shape with a width of 0.1–5 ms and the pulse rise and fall times shorter than 1 μs. The maximum pumping forward current pulse amplitude was 18 A. At the PL measuring the input window of the detector was covered with a Si filter to protect it from laser radiation. To excite the PL signal in the pulse mode of experiments, we used mainly a laser emitting at the wavelength $\lambda = 658$ nm (with the exception of some

special experiments). In some cases, we used a semiconductor laser emitting at the wavelength $\lambda = 0.98$ μm. Laser radiation was focused on the center of the sample to form a spot of diameter $d = 1$–1.5 mm. The laser pulses were rectangular in shape, the duration of the pulses was 0.6–1 ms, the rise time and decay time were shorter than 1 μs, and the repetition interval was 50 ms. The pulse duration chosen for the experiments practically provided the conditions for quasi-steady-state PL at the end of the pulse.

For determined η_{ext} at EL the LED radiation power was measured using a Ge photodiode (Hamamatsu B5170-50) with the known area S_{ph} and sensitivity K in the spectral range under consideration. The photodetector was situated at a distance of $L_{ph} = 25$ cm from the emitting surface and oriented perpendicular to this surface. The photodiode current Y_{ph} was measured, and the output radiation power was calculated using the formula

$$W = 2\pi {L_{ph}}^2 Y_{ph}/KS_{ph}M. \tag{2.3}$$

We introduced the empirical coefficient $M = 1.7$, which took into account the nonisotropic distribution of emission from a textured crystal surface within a hemisphere at a given distance L_{ph} from the LED. This coefficient was empirically determined from the results of measurements of Y_{ph} as a function of the angle between the normal to the sample surface and the direction to the sensitive area of the Ge photodetector [18].

The value η_{ext} was calculated as the ratio of the number of quanta (N_w) emitted by the LED per unit time ($N_w = W/h\nu_m$, where $h\nu_m$ is the quantum energy at the maximum of their energy distribution) to the number (N_{ing}) of minority carriers injected into the LED base per unit time ($N_{inj} = Y/q$, where Y is the forward current and q is the elementary charge). To determine the values of η_{ext} at PL we used the procedure described above, with the only difference being that the number of PL photons emitting per unit time was normalized to the number of photons of laser radiation (N_{ing}) incident on the sample surface per unit time ($N_{ing} = P/h\nu_L$), where P is the quasi-steady-state laser radiation power and $h\nu_L$ is the photon energy of laser radiation).

During measurements of the emission intensity distribution over the LED area, the samples were placed in the field of view of a microscope. The diameter of the microscope field of view on the emitting surface was about 0.5 mm. The germanium photodiode was placed in front of the eyepiece of the microscope.

When measuring the laser-induced free carrier absorption, the sample was illuminated from the front side by an incandescent lamp. On the opposite side of laser beam incidence, a germanium photodiode was placed, whose photodetecting area was covered by a thin (~0.5 mm) polished wafer of single-crystal germanium. Thus, the laser-induced free carrier absorption at wavelengths of the fundamental absorption edge of Ge was experimentally studied. The free carrier absorbance was determined by changes in the photodiode current during the laser irradiation pulses.

Analysis of the literature has shown that the c-Si LED with the highest efficiency and power was earlier described in [2]. This diode had a large emitting area of

~4 cm^2 (in fact, a forward-biased high-efficiency solar cell was used). At the highest currents studied in [2] (~0.2 A), the diode provided, according to our estimates, up to ~1.8 mW of power (W) emitted by the entire surface area of the diode and, accordingly, up to ~0.45 mW/cm^2 of average emitted power per unit area (P_0). In the present study, c-Si LEDs fabricated using the technology described in [2] were examined, but measurements were performed up to currents at which the decrease in the minority carrier lifetime, caused by Auger recombination, becomes important. Making the area of the structures smaller by cutting a larger area solar cell enabled a significant increase in P_0 and brought the emitting area closer to that typical of commercial LEDs of other types, whose emission can be readily focused (in contrast to that of large solar cells) on an illuminated object of a comparatively small-size photodetector area. Because of the increase in the working current, W could be substantially raised. In the present study the LEDs were produced from a silicon solar cell of dimensions 3.5 × 6 cm^2 fabricated on a single-crystal p-Si (~1 Ω cm) wafer. Its design and fabrication technology, described in [2], provided a combination of a low density of nonradiative recombination centers, low areas of n^+ and p^+ contacts, and special surface texturing for a considerable increase in the ratio between the external and internal quantum efficiencies of EL and PL [2]. In addition to the texturing and an antireflection coating, the face surface of the Si wafer contained thin heavily doped n^+ strips formed with a step of about 1 mm in parallel to the smaller side of the solar cell. From above, these bands were metallized and interconnected by a metallic busbar at the wafer edge. The Si LEDs studied were fabricated by cutting a solar cell. Most of the measurements were performed on three rectangular structures with faces parallel or perpendicular to the long sides of metallized n^+-layers. The structure with area $S_1 = 0.9 \times 0.95 = 0.85$ cm^2 (sample S_1) contained nine 9-mm-long metallized strips of n^+–p junctions which were not interconnected by a metallic busbar, in contrast to the structure described in [2]. The structure with area $S_2 = 0.4 \times 0.25 = 0.1$ cm^2 (sample S_2) corresponded in design to that shown in Fig. 2.1 of [2] and contained two metallized strips of n^+–p junctions connected by a metallic busbar. The area of the emitting (unmetallized) surface of this LED was $s = 0.055$ cm^2. We also have studied an LED structure of rectangular shape with an area of $S_3 = 12$ cm^2 (sample S_3) and the edges parallel and perpendicular to the long sides of metallized (3 cm long) n^+–p junctions not connected by a metal busbar. The use of such a long n^+–p junction allowed us to minimize the influence of nonradiative recombination centers formed along the cuts. In order to exclude the effect of such centers present near the lines of cutting parallel to the metalized n^+-bands, the measurement was performed on the n^+–p junctions spaced more than 1.5 cm from these lines.

PL together with free carrier absorption was studied using a non-textured n-Si wafer 0.35 mm thick thermally oxidized in dry oxygen (20 Ω cm), oriented in the (1 0 0) plane. Thermal oxidation passivated the silicon surface to prevent significant surface recombination.

In a number of experiments for studies of the edge luminescence laws industrial c-Si diodes in which the part of the case has been removed for a lead-out of radiation from edge area of diode have been used.

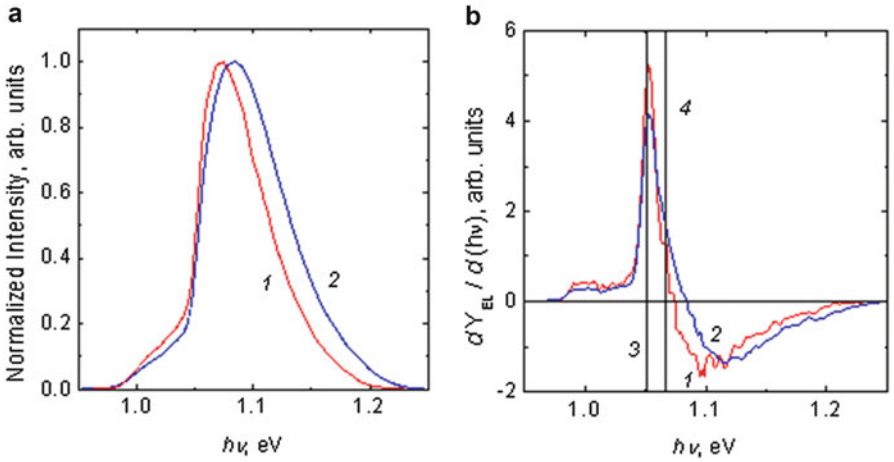

Fig. 2.1 Normalized spectra of the edge luminescence (**a**) and spectra for their derivatives (**b**) of c-Si at room temperature (294 K) for the diodes with surface texturing (*curve 1*) and without it (*curve 2*). The *vertical straight lines 3* and *4* indicate the photon energies which correspond to the absorption edge at 294 K involving single-TO phonons and with free exciton generation (*3*) and absorption edge involving single-TO phonons and with free carrier generation (*4*)

3 The Spectrum and Basic Laws of the Edge Luminescence in the Single-Crystal Silicon

Measured at relatively small currents (not causing heating of diodes) the normalized spectra of the edge luminescence of c-Si at room temperature (294 K) for the diodes with surface texturing by technology [2] (curve *1*) and without surface texturing (curve *2*) are submitted in Fig. 2.1a. A distinction of the curve *1* and the curve *2* is connected to various conditions of radiation exit. The basic edge luminescence peak of c-Si is commonly interpreted as being due to radiative recombination with emission of solitary transverse optical (TO) phonons. In addition, it is believed that a relatively minor contribution to the spectrum is made by radiative transitions with absorption of phonons, participation of two or larger number of TO phonons in recombination events, and participation of other phonons. In this work, we use the results of [23] as reference data. In [23] the band gap c-Si ($E_g = 1.1242$ eV at 300 K) as well as the temperature dependence of E_g were determined from the experimental absorption spectra of c-Si. The TO phonon energy emitted in the recombination event ($E_{ph} = 57.3$ meV for the basic peak) and the binding energy of free excitons ($E_{ex} = 14.7$ meV) were taken from [23] too.

In the work [17] the differential method of the analysis of spectra of the edge luminescence of semiconductors has been offered. It has allowed to show most evidently that the prevailing mechanism of edge radiative recombination in Si single crystals in a wide temperature region, including room temperature, is

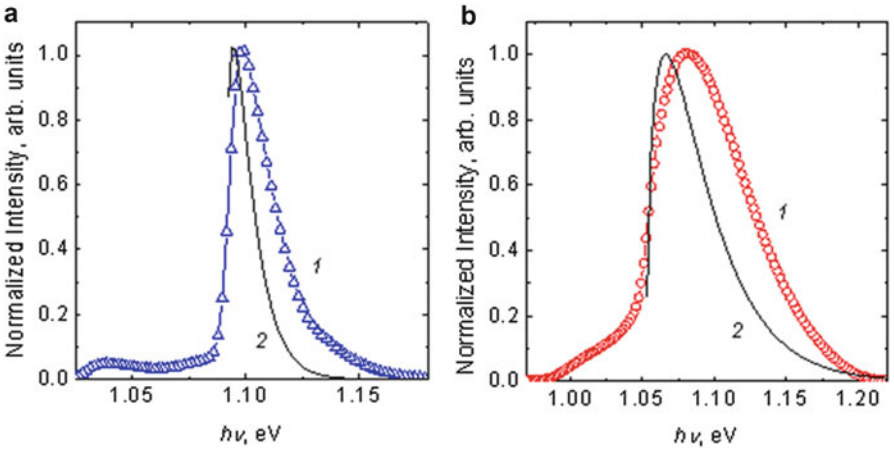

Fig. 2.2 The experimental edge EL spectra of c-Si (*1*) and the Maxwell distributions (*2*) with peaks at the absorption edges corresponding to the formation of free excitons and solitary TO phonons at $T = 80$ K (**a**) and $T = 300$ K (**b**) [17]

annihilation of free excitons. For the first time this conclusion has been made by the author of the present work in [15] and then confirmed by the experiments published in [16]. Figure 2.1b shows the spectra for the derivatives of the curves *1* and *2* from Fig. 2.1a. The vertical straight lines *3* and *4* indicate the photon energies which, according to the fundamental absorption measurements for c-Si [23], correspond to the absorption edge at 294 K involving single-TO phonons and with free exciton generation (2.3) and absorption edge involving single-TO phonons and with free carrier generation (2.4). According to the technique for analyzing the derivatives of the edge luminescence spectra, described below, the main spectral maxima observed are caused by the radiative recombination of free excitons in silicon involving TO phonons. Note that the dominant role of the radiative recombination in c-Si via free excitons near the temperature of liquid nitrogen is well known and needs no proof.

If edge radiative recombination is due to the annihilation of free excitons, the shape of the spectral curve is bound to be defined by the Maxwell distribution of the number of excitons n_{ex} with the kinetic energy E:

$$n_{ex}(E) = AE^{0.5}\exp(-E/kT). \tag{2.4}$$

Here, A is a coefficient independent of E, T is temperature, and k is the Boltzmann constant. The expression of the derivative dn_{ex}/dE, where n_{ex} is determined by (2.4), has a maximum at $E = 0$ (the derivative tends to infinity). Consequently, if the spectrum is described by formula (2.4), we can determine the photon energy corresponding to $E = 0$ from the position of the maximum of the derivative in (2.4). The experimental edge luminescence spectra of c-Si cannot be described by formula (2.4), at least at $T = 80$–300 K (see Fig. 2.2).

This may be caused by several factors, specifically (1) the self-absorption of emission in the short-wavelength region and (2) the superposition of some other peaks. In addition, as can be seen from (2.2), this can be attributed to the dependence of the radiative lifetime of excitons (τ_{ex}) on their kinetic energy. From (2.2), it is evident that the function $R(E)$ is similar to $n_{ex}(E)$ only if $\tau_{ex} = \text{const}$. However, the last mentioned condition seems to be rather improbable, since for the radiative recombination event to occur in indirect-gap semiconductors in certain conditions, it is necessary that the exciton should interact with a phonon (or an impurity atom, as in the case of the SiGe alloy). However, the probability of satisfying these conditions is bound to depend on the exciton kinetic energy. To date, the dependence $\tau_{ex}(E)$ practically has not been studied. Therefore, whether or not the position of the maximum of the derivative of the $R(E) = n_{ex}\ (E)/\tau_{ex}(E)$ spectral curve coincides with the photon energy corresponding to $E = 0$ can be judged only from comparison of the experimental position of this maximum with the experimentally determined absorption edge for free excitons. This is what is done in this study. In accordance with (2.2), the derivative dR/dE is described by the expression

$$dR/dE = (dn_{ex}/dE)/\tau_{ex} - n_{ex}(d\tau_{ex}/dE)/{\tau_{ex}}^2. \tag{2.5}$$

As follows from the analysis of formula (2.5), the position of the maximum of dR/dE can be inconsistent with $E = 0$ if $\tau_{ex}(E = 0)$ is infinitely large. Infinitely large $\tau_{ex}(E = 0)$ would mean that the radiative annihilation of excitons with $E = 0$ is practically impossible. To date, this effect has not been theoretically understood. It can lead to shift of the maximum of the derivative in the direction of high photon's energy. The absence of such significant shift under different conditions of the emission output of the samples (Fig. 2.1b) indicates that at using of the differential method of analysis of the luminescence spectra this effect can usually be ignored. Such coincidence of the positions of the maximums of the derivative with the absorption edge defined by free excitons and the lack of pronounced maximums near the intersections of curves *1* and *2* with straight lines *4* on Fig. 2.1b support the conclusion [15] that the prevailing mechanism of radiative recombination in c-Si at room temperature is the phonon-assisted radiative annihilation of free excitons. The above model notions require that τ_{ex} would be smaller by more than two orders of magnitude than the radiative lifetime of free charge carriers (τ_f). Such a considerable difference between τ_{ex} and τ_f can be related to the fact that the average distance between free carriers in the experiments was more than Bohr radius of exciton ($r_B = 4.2$ nm). In addition, radiative recombination in c-Si requires a certain correlation in the mutual arrangement of electron, hole, and phonon, which is most probably realized in the case of recombination via excitons.

The authors of [24–26] drew a similar conclusion for the prevailing mechanism of edge radiative recombination in SiGe alloys. Previously, the conclusion that the prevailing mechanism of edge luminescence at room temperature is annihilation of free excitons was drawn in a study of the luminescence spectra of another semiconductor, GaP [27]. In [28], it was proved that, at room temperature, radiative recombination in the region of the fundamental absorption edge of silicon carbide

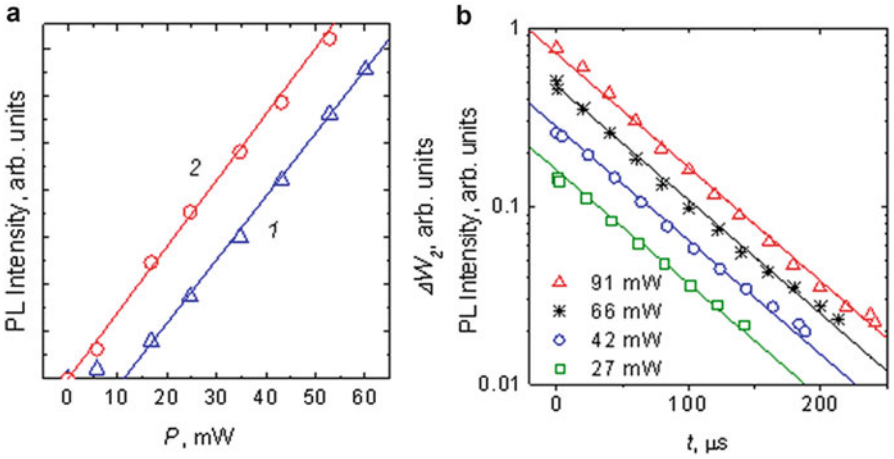

Fig. 2.3 (**a**) Dependences of the total intensity of the edge PL (*1*) and radiation absorption in the sample by free carriers ΔW_2 on the laser radiation power P incident on the sample (*2*) [21]. (**b**) Measured at different P the kinetics of the PL intensity decay in the linear region of the dependence of the PL intensity on P

occurs via annihilation of free excitons. All semiconductors explored in the abovementioned studies are indirect-gap materials with binding energies of free excitons ~6 meV and higher. From the aforesaid studies, we can infer that, in the region of the fundamental absorption edge of all indirect-gap semiconductors with no defect-related luminescence, radiative recombination via the annihilation of free excitons prevails in a wide temperature range, including room temperature (in spite of the relatively low concentration of excitons, as compared to the concentration of free charge carriers at room temperature).

In the work [21] the edge PL intensity and the change of absorption by free charge carriers, depending on the power (P) of the laser radiation causing these effects, were measured in the same place of the thermally oxidized c-Si. Figure 2.3a (data *1*) shows the dependence of the structure's edge PL intensity on the laser radiation power incident on the sample. We can see the almost linear dependence of the edge PL intensity on P but only after the initial superlinear region. The kinetics of the order of magnitude decay of the PL in the linear region of the dependence of the PL intensity on P was approximated by an exponential function with a time constant, which was almost independent of P (Fig. 2.3b).

In [21] the dependences of the number of laser-induced free minority carriers on P were studied. To this end, the absorbance of infrared radiation from the silicon conduction band by free carriers was measured. The data of such measurements were processed using the theory published in [29] and improved by the author, taking into account features of the present experiments. The radiation power W_0 incident on the sample from the region of the fundamental absorption edge of germanium is related to the power W_1 passed through the wafer as

$$W_1 = W_0(1-R_1)(1-R_2)\exp(-kL)\left[1+R_2{}^2\exp(-2kL)\right], \tag{2.6}$$

where R_1 is the reflectance from the outer sample surface, R_2 is the reflectance of radiation incident on the silicon surface from the inside, L is the silicon wafer thickness, and k is the effective absorbing coefficient by free carriers. Expanding the exponential functions in expression (2.2) in series, taking into account the smallness of kL (<0.005 according to estimations), we obtain

$$\begin{aligned} W_0 - W_1 &= W_0\left[1-(1-R_1)\left(1-R_2\right)\left(1-kL\right)\right]\left[1+R_2{}^2-kL2R_2{}^2\right] \\ &= \Delta W_1 + \Delta W_2\left(kL\right) = \Delta W_1 + W_0(1-R_1)\left(1-R_2\right)\left(1+3R_2{}^2\right)kL. \end{aligned} \tag{2.7}$$

According to the above conditions for measuring the free carrier absorbance, the quantity ΔW_2 caused by free carrier generation is proportional to the Ge photodiode photocurrent pulse amplitude measured using an oscilloscope under pulsed laser exposure. As can be seen from (2.7), the quantity ΔW_2 is also proportional to kL. The results of experimental studies are shown in Fig. 2.3a (dependence *2*). The quantity ΔW_2 caused by free carrier generation almost linearly depended on P in the whole studied P range. The theoretical expression for kL considering the nonuniform distribution of free carriers over the silicon wafer thickness is given by [29]

$$kL = \int_0^L \alpha(x)\mathrm{d}x, \tag{2.8}$$

where α is the absorbing coefficient of free carriers and x is the distance from the irradiated Si surface. The value of α is determined by the formula [29]

$$\alpha(x) = \sigma_{n+p}\Delta p(x), \tag{2.9}$$

where $\Delta p(x)$ is the change in the hole concentration due to laser irradiation, $\sigma_{\mathrm{n+p}}$ is the total cross section of electron and hole absorption at the probe light wavelength, and $\sigma_{\mathrm{n+p}} = 2 \times 10^{-17}$ cm^2 for the spectral composition of the light (1.8–2.5 μm) used in [28], which is close to that in the Ge fundamental absorption edge region used in this study. The kinetic measurements of the carrier lifetime in the sample under study allowed us to determine the carrier diffusion length (L_p) which was approximately equal to the silicon wafer thickness. In view of this fact and the circumstance that the penetration depth of a major fraction of the used laser beam radiation into silicon did not exceed 1 % of this value, we calculated $\Delta p(x)$ using the formula [30] describing the carrier distribution over the thickness of the thin diode base with a blocking contact to the base:

$$\Delta p(x) = \Delta p_1 \cosh\left[(x-L)/L_p\right]/\cosh\left(L/L_p\right), \tag{2.10}$$

where Δp_1 is the concentration of free holes (generated by the laser beam in this study) near the silicon surface, where $x = 0$. Substituting (2.10) and (2.9) by (2.8), we obtain

$$kL = \sigma_{n+p}\,\Delta p_1 L_p \tanh\left(L/L_p\right). \tag{2.11}$$

According to [30], Δp_1 can be determined by the formula

$$\Delta p_1 = \beta P L_p / D_p, \tag{2.12}$$

where β is the coefficient independent of L_p and D_p is the hole diffusion coefficient. Then, substituting (2.12) by (2.11), taking into account $L_p = (\tau_p D_p)^{0.5}$, we obtain

$$kL = \sigma_{n+p}\beta P \tau_p \tanh\left[L/\left(D_p\tau_p\right)^{0.5}\right]. \tag{2.13}$$

Thus, if ΔW_2 (and, according to (2.7), kL) depends linearly on P, the linear behavior of recombination follows from (2.13), at which the hole lifetime τ_p is independent of P. The linear behavior of recombination is also independently confirmed by measurements of the PL decay kinetics in the linear portion of curve *1* in Fig. 2.3a. Since the time of reaching the equilibrium exciton concentration is significantly smaller than τ_p, the independence of the order of magnitude decay time constant for the PL intensity of P means also the τ_p independence of P. In the case of the linear behavior of recombination, it follows from (2.10), (2.12), and

$$P = \gamma \int_0^L \Delta p(x)\mathrm{d}x/\tau_p \tag{2.14}$$

(where γ is a factor) that $\Delta p(x)$ are proportional to P. At the same time, it follows from the above that $n_{ex}(x)$ are also proportional to P. Indeed, at the same n_{ex}, the edge PL power entering the photodetecting area from the unit volume depends on the distance between the emitting volume and the sample surface. This is due to edge PL self-absorption in silicon. The unchanged shape of the normalized PL spectrum as P varies in the linear portion of curve means that a change in the distribution function of free excitons with P is reduced to only a proportional change in $n_{ex}(x)$ for all distances from the sample surface. Accordingly, $n_{ex}(x)$ are proportional to $\Delta p(x)$. Figure 2.4 shows the results of studies at room temperature the edge EL of the industrial diode with area of ~3 mm^2 and a donor impurity concentration in the base ~10^{14} cm^2. We can see the almost linear dependence of the edge EL intensity on current after the initial superlinear region. According to Fig. 2.4b on the linear portion of the dependence the lifetime of the charge carriers is independent of the intensity of the luminescence excitation (current value). At sufficiently high currents after the linear region sublinear region, in which

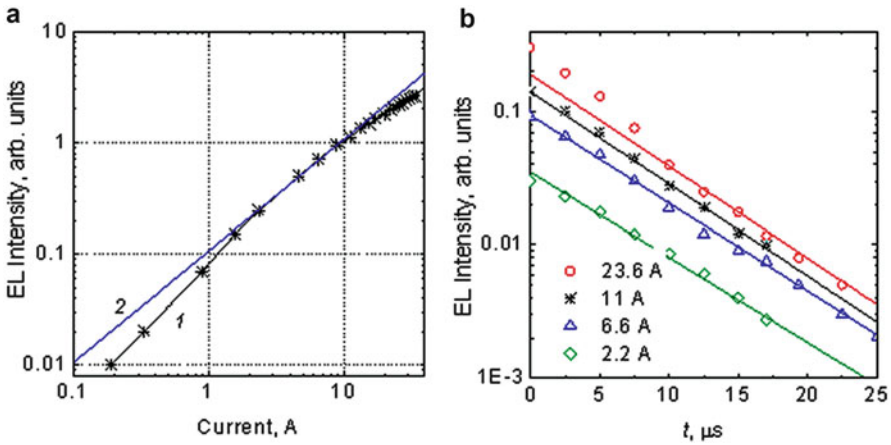

Fig. 2.4 The dependences of EL intensity of the c-Si LED on the forward current (**a**) and at different currents on the time after the current was cut off (**b**). *Straight line 2* in (**a**)—approximation of section of the experimental curve *1* by linear fit

there is a more rapid initial intensity decay kinetics of EL, is observed. This may be due to the fact that at such currents in addition to Shockley–Read–Hall recombination Auger recombination begins to have a significant influence.

It is well known that for low injection levels, when the concentration of minority carriers injected from the p–n junction or generated by radiation is significantly lower than the dopant concentration, explanation of the linear regions within the existing theoretical concepts does not present difficulties. But according to the author's estimations, the close-to-linear dependence of the PL intensity on P and EL intensity on current (accordingly, n_{ex} on $\Delta p(x)$) in the samples under study began at average hole concentrations of ~(1–2) $\times$ 10^{16} cm^{-3}. Because the specific resistance of thermally oxidized n-Si wafer was 20 Ω cm and donor impurity concentration in the LED's base ~10^{14} cm^2, at such concentrations conditions of high injection levels (when the concentration of minority carriers is significantly higher than the dopant concentration) took place. The above results showed that the linear or the close-to-linear portions of the dependences of the edge luminescence intensity of c-Si on the luminescence excitation intensity under conditions of high injection levels are caused by radiative recombination predominantly via free excitons and by the existence of linear or close-to-linear portions of the dependences of the free exciton concentration on free carrier concentration at the sufficiently high free carrier concentrations. The results presented show that at sufficiently high concentrations of free charge carriers (for example, greater than ~(1–2) $\times$ 10^{16} cm^{-3}), (2.1) cannot be used to describe the rate of radiative recombination in c-Si. According to the experiments in this case the dependence of the rate of radiative recombination on the concentration of free electrons or holes should be described by a linear function and does not depend on the concentration of free charge carriers of opposite sign. Note also that as calculated in [13]

dependence of B on the concentration of free charge carriers does not explain the linear sections of the dependences of the EL and PL intensity on the excitation intensity, as it is not sufficiently strong. Similarly, the effect of screening taking into account that in [14] is not sufficiently strong to explain the experimental results. The presented results of researches allow to expand opportunities of luminescent methods of definition of c-Si parameters (for example, τ and L_D) on the area of high levels of injection and high intensities of the luminescence excitation. Earlier it was impossible due to the lack of the adequate description of the dependence of the radiative recombination rate R on the concentrations of free charge carriers for considered area of free charge carrier concentrations.

4 Near-Band-Edge Electroluminescence in Silicon Light-Emitting Structures Fabricated Using High-Efficiency Solar Cell Technology

Figure 2.5 shows EL spectrums of the diode S_2, measured at room temperature (a) and 80 K (b), at different forward currents and normalized to the maximum intensity. At room temperature up to currents ~6.5 A, changes in the spectrum upon an increase in the current are insignificant. An analysis of the long-wavelength part of the EL spectrum at the currents not more than 6.5 A demonstrated the predominance of the TO phonon-assisted radiative recombination of free excitons. The distortion of the spectrum at the current of 10 A is possibly due to heating of the sample by the flowing current. In addition, the mechanism of radiative recombination can change at sufficiently high free carrier concentrations: the radiative recombination of an electron–hole plasma may become important.

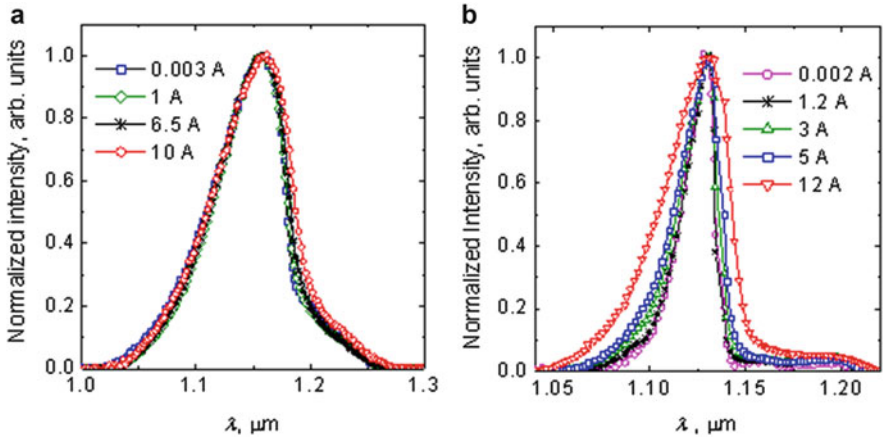

Fig. 2.5 EL spectrums of the diode with area S_2, measured at different forward currents at room temperature [18] (**a**) and 80 K [22] (**b**)

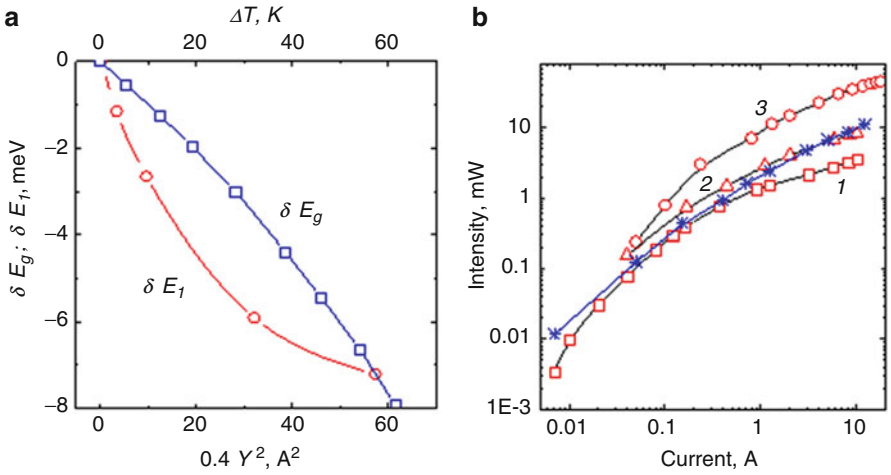

Fig. 2.6 (**a**) Difference (δE_1) between the photon energy corresponding to half the maximum of the normalized EL intensity on the long-wavelength side of the peak and the value of this photon energy at a current of 0.002 A as a function of the square of current (Y^2) and the dependence of the change (δE_g) in the band gap width of c-Si on the increase (ΔT) in temperature relative to 80 K (data from [23]). (**b**) Current dependence of the integrated LED edge EL power measured at 300 K (1–3) and 80 K (4). 1,4—to sample S_2, 2—to sample S_1, 3—to sample S_3 (data from [18, 19, 22])

At 80 K the position of the maximum of the wavelength distribution (λ_{max}) is almost the same over the entire range of currents studied. The half-width of the spectra also remains almost unchanged for currents $Y \leq 1.2$ A. At currents exceeding 1.2 A, the spectra are significantly broadened and, accordingly, the area under the spectral curves (S_{sp}) increases. At a current of 12 A, the area under the spectral curve in Fig. 2.5b is approximately twofold greater than that at currents smaller than 1.2 A. The wavelength $\lambda_{max} = 1.13$ μm and the spectral half-width 0.018–0.020 μm (at currents smaller than 1.2 A) coincide (to within experimental error) with the respective quantities measured earlier for Si LEDs without a surface texture. Such EL peaks are usually interpreted as being due to radiative recombination of free excitons in c-Si with the formation of a single-TO phonon. In addition, the EL spectrum contains relatively small contributions from radiative transitions of excitons with absorption of a phonon and with involvement of two or more TO phonons and other phonons. At currents exceeding 1.2 A, the EL spectra are observed to broaden to both longer and shorter wavelengths and the broadening increases with current. Figure 2.6a shows the difference (δE_1) between the photon energy corresponding to half the maximum of the normalized EL intensity on the long-wavelength side of the peak and the value of this photon energy at a current of 0.002 A as a function of the square of current (Y^2). The difference δE_1 increases with the square of current following a sublinear law. The reason why the quantity δE_1 is plotted as a function of the square of current will become apparent later on. We have shown that the broadening of the EL spectra of the high-efficiency c-Si

LED studied is caused by the change of the EL mechanism rather than by the heating effect of the current passing through the LED. Indeed, the contribution of heating to the spectrum broadening can be revealed by analyzing the c-Si EL spectra at different temperatures (see, e.g., [2]). As the temperature of c-Si LEDs increases above 80 K, the EL spectra are usually broadened to both shorter and longer wavelengths. The broadening to longer wavelengths is usually due to a decrease in the band gap width (E_g) of silicon. According to [22], the change in E_g (Fig. 2.6a) and the change in the photon energy corresponding to half the maximum of the normalized EL intensity on the long-wavelength side of the peak (at least in the range 80–200 K) exhibit a superlinear dependence on the increase in temperature relative to 80 K (Fig. 2.6a). However, according to theoretical estimates [31], the current dependence of the difference between the temperature of an LED attached to a cold finger and the temperature of the cold finger follows a square law. Therefore, the sublinear dependence of δE_1 on the square of current and, hence, on temperature (Fig. 2.6a) is inconsistent with the assumption that the broadening of the EL spectra is due to the heating effect of the current passing through the LED. This assumption is also inconsistent with the small duration of current pulses, the large pulse period-to-pulse duration ratio, and good heat-removing conditions.

It was shown in [22] that the mechanism of radiative recombination can change at sufficiently high free carrier and exciton concentrations: the radiative recombination of an electron–hole plasma may become important. Figure 2.6b shows the integrated radiation power (over the entire spectral range studied) emitted by an LED at 300 and 80 K into a hemisphere as a function of current. The initial small nonlinear segments are seen to be followed by an almost linear dependence, which, in turn, is followed by long sublinear segments. At 80 K and a maximum current of 12 A, the LED radiation power $W = 11$ mW. This value corresponds to a record area-averaged radiation power per unit surface area $P_0 = 0.2$ W/cm^2 for c-Si LEDs (edge luminescence and other types of luminescence), which is more than threefold greater than the value of P_0 obtained for the same LED at 300 K at a pulsed current of 10 A [2]. At the same current (10 A), the value of P_0 at 80 K is also almost threefold greater than that at 300 K. Pumped by a pulsed current of 18 A, the LED S_3 (see graph 4 in Fig. 2.6b) showed a record high power of the near-band-edge electroluminescence at room temperature (~46 mW).

The current dependences of the external EL quantum efficiency that measured the samples at 80 and 300 K are presented in Fig. 2.7a. These curves are seen to exhibit a maximum. The reasons why the efficiency η_{ext} decreases with increasing current at 300 K were analyzed in [18]. It was shown in [18] that the decrease in η_{ext} with an increase in current is mainly due to the occurrence of Auger recombination, which is added to nonradiative recombination by the Shockley–Read–Hall mechanism operating at smaller currents as well. This assumption is confirmed by data on the kinetics of EL decay at various currents, which are presented in Figs. 2.7b and 2.8. For the maximum η_{ext} the EL intensity decay by an order of magnitude is well described by an exponent with a characteristic decay time (τ_d) (maximum of 380 μs for sample S_3, Fig. 2.8b, curve). On the descending parts of the η_{ext} curves, the EL

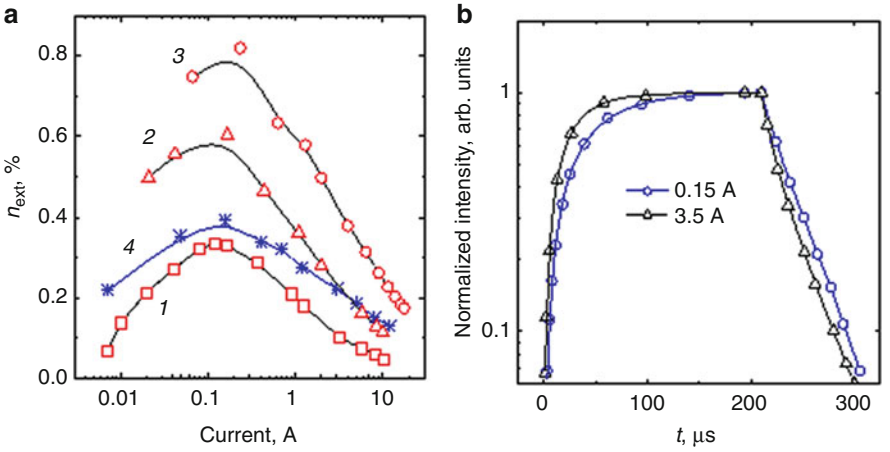

Fig. 2.7 (**a**) Current dependences of the LED external quantum efficiency measured at 300 K (1–3) and 80 K (4). 1,4—to sample S_2, 2—to sample S_1, 3—to sample S_3. (**b**) LED EL kinetics at 80 K for two different values of the current (to sample S_2) [22]

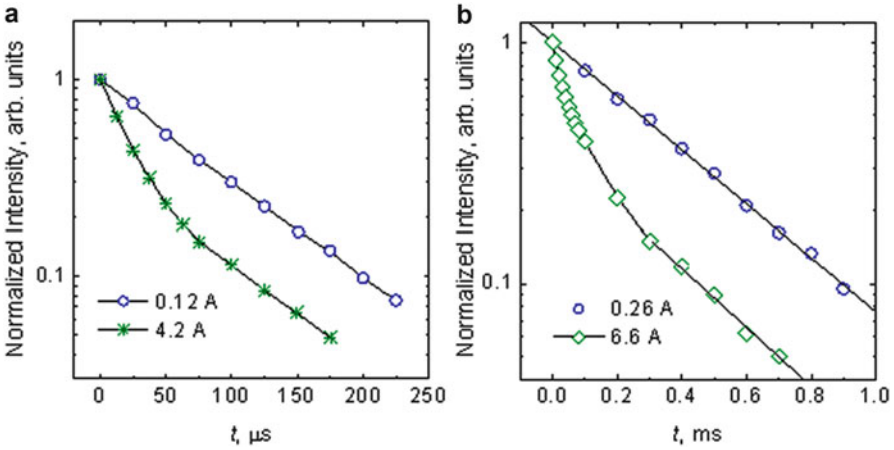

Fig. 2.8 LED EL kinetics at 300 K for two different values of the current: (**a**) to sample S_1 [18], (**b**) to sample S_3 [19]

intensity decay kinetics is described by an exponent with the same τ_d only after the initial, more rapid decay (Figs. 2.7b and 2.8, curves *2*), that is, after a decrease in the carrier density to a level where the Auger recombination becomes insignificant. Another reason (apart from Auger recombination) for the observed behavior of η_{ext} with increasing current at 80 K is the significant broadening of the EL spectra, as seen from Fig. 2.5b. As can be seen from Figs. 2.6b and 2.7a, the area of the sample by means of its cutting decreases significantly radiating power and the external EL quantum efficiency of the LEDs. This may be connected with formation of the

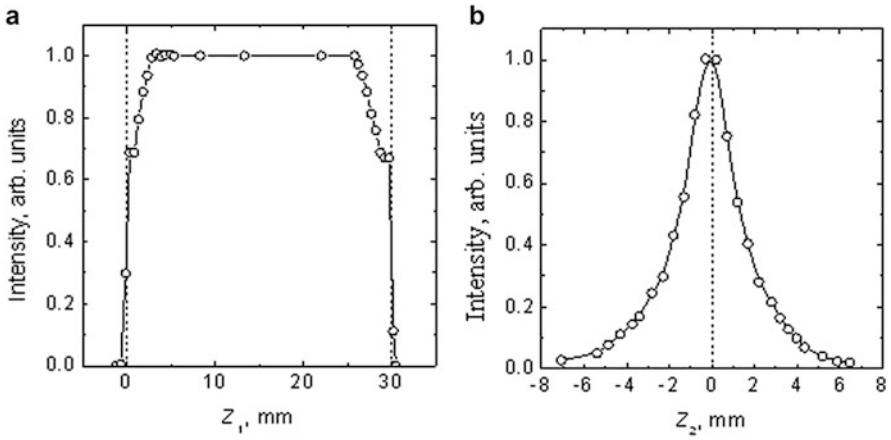

Fig. 2.9 Normalized distribution of the near-band-edge EL relative to the axis along (**a**) and perpendicular (in the *center*) (**b**) to the long side of the n^+–p junction [19]

centers of nonradiative recombination near the lines of cutting. The influence of the nonradiative recombination near the lines of cutting appears in EL intensity decay near the lines of cutting (see Fig. 2.9a). EL intensity decay perpendicular to p–n junction in Fig. 2.9b is determined by diffusion length of minority charge carriers and by lateral extension of radiation in the sample.

5 The Edge Photoluminescence and Nonradiative Recombination in Single-Crystal Silicon with a p–n Junction: Structures Produced by High-Efficiency Solar Cell Technology

The studies of the edge PL were made at room temperature for the structure of the design which corresponded to that shown in Fig. 2.1 in [2]. The nonmetallized surface area of the structure was $S_4 = 0.3 \times 0.4 = 0.12$ cm^2. Laser radiation was focused on the center of the sample to form a spot of diameter $d = 1$ mm. Figure 2.10a illustrates the kinetics of the edge PL at different laser radiation powers P at the laser wavelength $\lambda = 658$ nm. The experimental points corresponding to the rise in the PL intensity with time (t) well fit the dependence

$$Y_{\mathrm{PL}} = Y_{\mathrm{PL\ max}}[1 - \exp(-t/\tau_{\mathrm{r}})], \tag{2.15}$$

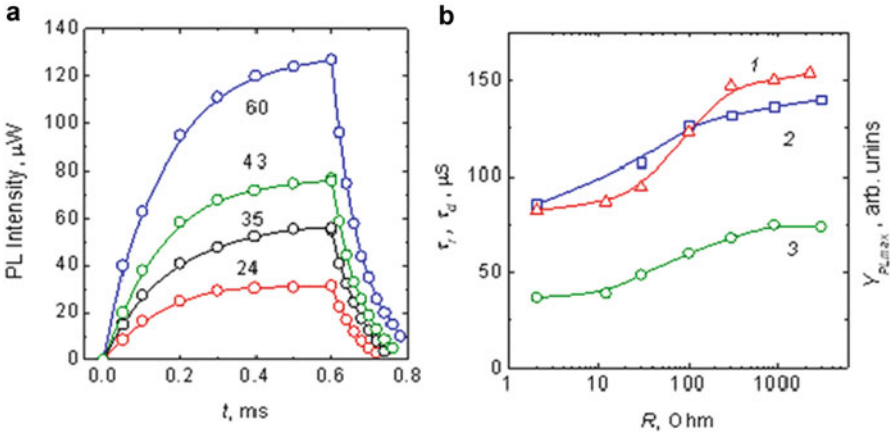

Fig. 2.10 (**a**) The kinetics of PL at zero external voltage and at different laser radiation powers (expressed in mW and indicated near curves). (**b**) Dependences of the quasi-steady-state PL intensity Y_{PLmax} and the PL rise and decay time constants τ_r and τ_d on the bypass resistance R ($P = 60$ mW) [20]

where τ_r is the rise time constant and $Y_{PL\ max}$ is the quasi-steady-state PL intensity. The portions of experimental curves corresponding to the PL decay can be described by the expression

$$Y_{PL} = Y_{PL\ max}\exp(-t/\tau_d), \tag{2.16}$$

where τ_d is the decay time constant. In Fig. 2.10a, the quantities τ_r and τ_d differ widely in magnitude. The value of τ_r is practically independent of P and corresponds to ~140 μs. In the range of laser radiation powers used in the study, the value of τ_d increases with P from ~60 to ~75 μs. According to formula (2.15), the value of τ_r corresponds to the time ($\tau_{0.63}$), in which the increasing PL intensity reaches approximately a 0.63 fraction of the maximum intensity [32]. A considerable excess $\tau_{0.63}$ of over τ_d has been already observed in the previous studies of edge EL in Si-based LEDs [33]. However, in [33], this difference was attributed mainly to the time delay of establishment of the quasi-steady-state current. Such an interpretation is inapplicable to the results of this study, since the quasi-steady-state laser radiation intensity is achieved here in a time shorter than 3 μs. In order to gain an insight into the causes of the large difference between τ_r and τ_d, we carried out experiments in which forward and back DC voltages were applied across the structure simultaneously exposed to pulsed laser radiation. Modulation of the quasi-steady-state edge PL intensity in such a structure under variations in the voltage across the p–n junction was first demonstrated elsewhere [34]. Upon application of voltages, the p–n junction of the structure is bypassed to a certain extent by the internal resistance of the voltage source. For this reason, we initially studied the effect of the bypassing resistance (R) on the parameters of PL of the structure.

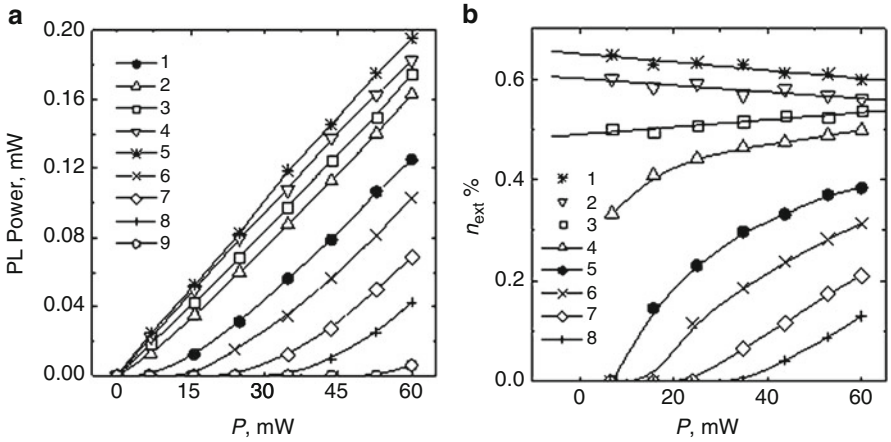

Fig. 2.11 (**a**) Plots of PL pulse power versus exciting laser radiation power P at $\lambda = 658$ nm for various direct currents: 0 (*1*), 6 (*2*), 9.3 (*3*), 16 (*4*), and 22.6 mA (*5*) and reverse-bias voltages: 0 (*1*), 4.2 (*6*), 9.3 (*7*), 12.8 (*8*), and 17.6 V (*9*) [34]. (**b**) Plots of the external quantum efficiency η_{ext} versus exciting laser radiation power P for various direct currents: 22.6 (*1*), 16 (*2*), 9.3 (*3*), 6 (*4*), and 0 mA (*5*) and reverse-bias voltages: 0 (*5*), 4.2 (*6*), 9.3 (*7*), and 12.8 V (*8*) [34]

Figure 2.10b shows the dependences of the PL intensity and the quantities τ_r and τ_d on R at $P = 60$ mW. From Fig. 2.10b, it can be seen that, as R is decreased to values smaller than 1 kΩ, the PL intensity $Y_{PL\ max}$ and the time constants τ_r and τ_d drastically decrease. Therefore, in all of the experiments described below, the internal resistance of the voltage source was chosen in the range 1.2–1.4 kΩ. Connection of such resistance only negligibly changed the PL intensity.

Figure 2.11a (curve *1*) shows the dependence of the quasi-steady-state edge PL peak intensity on P at zero external voltage and $\lambda = 658$ nm. In these conditions, the quasi-steady-state PL external quantum efficiency steadily increases with P, starting from some threshold value of P and tending to saturate at $\eta_{ext} = 0.4$ % (the dependences η_{ext} (P) at different forward currents and back voltages are shown in Fig. 2.11b). In curve *1* in Fig. 2.11a, we can distinguish three portions. In the first portion, no PL signal was detected at the achieved sensitivity level of the recording system. Starting from some threshold value of P, the PL intensity $Y_{PL\ max}$ first increases superlinearly with P and then approaches a practically linear dependence. Estimations show that, for the structure and the experimental system used here, the quasi-steady-state PL technique in the mode of measuring described in publications cannot be applied to the determination of the effective lifetimes at laser radiation densities lower than ~1 W cm^2 primarily because of the lack of the PL signal. Figure 2.11a shows also the dependences of the PL intensity on the laser radiation power P at four forward currents (curves *2*–*5*). With increasing forward current, the threshold power P at which the PL signal becomes evident decreases and the dependences $Y_{PL\ max}$ (P) become more and more closer to linear functions. Correspondingly, the quantum efficiency η_{ext} increases (see Fig. 2.1b). At the current

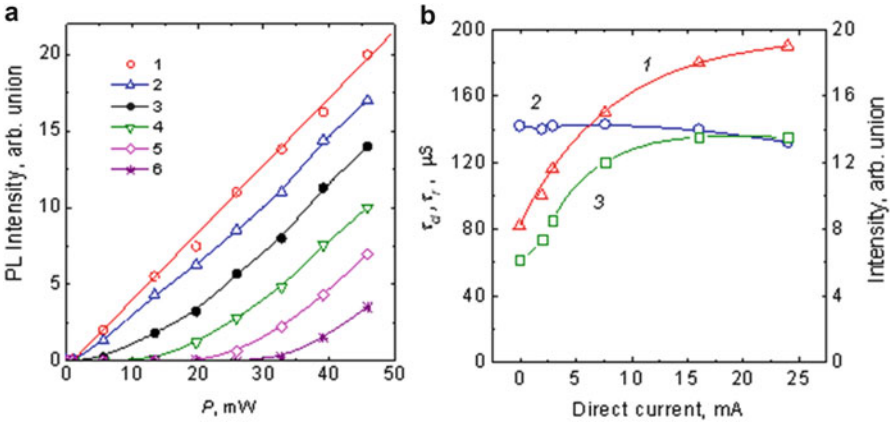

Fig. 2.12 (**a**) Dependences of the quasi-steady-state PL intensity on the laser radiation power at $\lambda = 0.98$ μm. *Curves 1–6* refer to the dependences at (*3*) zero external voltage, (*1*, *2*) the forward currents (*2*) 7.5 and (*1*) 24 mA, and (*4*, *5*, *6*) the reverse voltages (*4*) 7.5, (*5*) 14.5, and (*6*) 20 V [20]. (**b**) Dependences of the quasi-steady-state PL intensity (*1*) and the PL rise (*2*) and decay (*3*) time constants on the forward current for sample S_4 [20]

23 mA, η_{ext} is almost independent of P and corresponds to ~0.6 %. A DC reverse voltage applied to the sample decreases the PL intensity (see curves *6–9* in Fig. 2.11b) and, correspondingly, the quantum efficiency η_{ext}. In this case, the threshold power P behaves inversely: it increases, and the increase is more noticeable at higher reverse voltages. As the reverse DC voltage is increased, we observe a decrease in the PL decay time constant. Based on the results of studies of edge EL in c-Si [35], the author of [34] suggested that one of the possible causes of the effect of modulation of the edge PL, when excited by laser radiation at the wavelength $\lambda = 658$ nm, under variations in the voltage across the p–n junction was a change in the width of the SCR. It was noted that this effect could be due to the fact that the excitation radiation intensity became e times lower in intensity at a small depth (about 2.5 μm) comparable to the SCR penetration depth. To verify this assumption, we studied the effect of modulation of the edge PL power in c-Si by varying the voltage across the p–n junction on excitation of PL by laser radiation at $\lambda = 0.98$ μm. In c-Si, radiation at this wavelength is attenuated by a factor of e at a much larger depth (about 100 μm). The results are shown in Fig. 2.12a. The results are qualitatively similar to those shown in Fig. 2.11a. Consequently, the penetration depth of laser radiation in the samples is of no principal significance for observation of the effect of modulation of edge PL.

Figure 2.12b shows the dependences of the quasi-steady-state PL intensity and the PL rise and decay time constants on the forward current for the sample exposed to laser radiation pulses ($P = 35$ mW). From the results shown in Fig. 2.12b, it follows that the increase in the PL intensity correlates with the increase in the decay time constant τ_d. The time constant τ_d is larger at lower recombination rates of nonequilibrium charge carriers generated by laser radiation. Consequently, from

the results, it follows that the forward current slows down the recombination processes in the structure when responding to laser radiation pulses and, thus, increases the amplitude of PL pulses. It should be noted that, as the forward current is increased, the time constant τ_r changes only slightly; at rather large currents, the values of τ_d and τ_r practically coincide.

The effects observed at different forward currents can be understood in the first approximation, if it is assumed that there are two recombination channels in the structure. Moreover, it must be assumed that one of the channels is much less efficient than the other and the nonradiative recombination rate in the second, more efficient channel ceases to depend on the concentration of nonequilibrium charge carrier at sufficiently high concentrations. If these assumptions are accepted and the radiative recombination rate is negligible compared to the nonradiative recombination rate (because of the relatively low quantum efficiency of radiative recombination), the rate of changes in a number of nonequilibrium minority charge carriers generated by laser radiation (N) can be described in the first approximation by the expression

$$dN/dt = G - N/\tau - F. \tag{2.17}$$

Here, G is the rate of generation of minority charge carriers by laser radiation, N/τ is the rate of nonradiative recombination via the first mechanism (Shockley–Read–Hall mechanism), and F is the rate of nonradiative recombination of nonequilibrium charge carriers via the second mechanism. In the subthreshold conditions, the quantities G and N are small (because of the fast recombination of charge carriers mainly through the second channel), and, hence, the PL intensity is low. If the quantity G is sufficiently large and, therefore, the quantity F rapidly becomes practically constant, from formula (2.3) it follows that the time variations in N are described by the expression

$$N = N_{max}[1 - \exp(-t/\tau)], \tag{2.18}$$

where N_{max} is a maximum number of minority charge carriers at a specified generation rate G. If laser radiation is turned off ($G = 0$) and there is no forward current, there is no source of minority charge carriers to provide saturation of recombination via the second mechanism; then the rate F can depend on t, as can be seen from (2.17), and the decay time constant for the quantity N can be smaller than τ. However, if a rather large forward DC current passes through the sample, the second recombination channel for optically generated charge carriers is turned off by nonequilibrium charge carriers generated by the current passing through the p–n junction. In this case, from (2.3) it follows that the decay kinetics of minority charge carrier number generated by laser radiation is described by the expression

$$N = N_{max}\exp(-t/\tau). \tag{2.19}$$

It should be noted that, in this case, the rise and decay time constants for N are practically identical and equal to τ, since the quantity F for optically generated charge carriers in formula (2.17) must be assumed to be zero also for the rise of the PL intensity. Upon application of a reverse voltage, the external field separates charge carriers, resulting in an acceleration of the kinetics of PL and in a decrease in the PL intensity. In the foregoing, we considered the kinetics of changes in the concentration of optically generated free minority charge carriers in the structure under study. However, as reported previously, radiative recombination in c-Si at room temperature occurs basically through the formation of free excitons and, correspondingly, the PL intensity depends on the concentration of excitons (N_{ex}) in accordance with the formula

$$Y_{PL} = C_1 N_{ex}/\tau_{ex}. \tag{2.20}$$

Here, C_1 is a constant. The problem of interconnection between the kinetics of free excitons and that of free charge carriers was discussed elsewhere [36]. It was shown that the description of the kinetics of annihilation of excitons led to a nonlinear second-order differential equation that has not yet been solved in the general case. On the assumptions accepted in [36], it was found that, in the case of radiative recombination via free excitons, the quantity τ_d was half the quantity τ. For the qualitative consideration presented here, it is important that the faster (or slower) the kinetics of N, the faster (or slower) the kinetics of N_{ex}. This conclusion can be drawn on the basis of the results of [36] as well as from the value of the time of binding of free charge carriers into excitons. The last-mentioned time is several orders of magnitude shorter than τ_d and τ_r. Therefore, at a qualitative level, the above analysis of the kinetics of N can be used to interpret the systematic features of the kinetics of N_{ex} and, hence, the kinetics of PL in different experimental conditions.

It was of importance here to understand to what extent these effects are inherent in high-efficiency Si solar cells described in [2]. The answer to this question can be obtained from comparison of the data presented above with the data reported in [37]. In [37], the quantum efficiency of a solar cell similar to that considered here reached the slightly varying level at EL excitation intensities of about 0.1 mW cm^{-2}. These intensities are several orders of magnitude lower than the PL excitation intensities observed for the structure studied here. Thus, the above-described effects as such and their manifestation in high-efficiency solar cells may be a consequence of specific features of the solar cell technology, variations in the manufacturing process, and cutting of elements to form separate parts; the last-mentioned procedure brings about the formation of new recombination centers. It is important to note that the basic objective laws of the second channel of nonradiative recombination of the edge PL described above are qualitatively similar to those obtained in studies of edge PL in sample S_3 at least 1 cm away from the cut line. This means that the described effect of the second channel of nonradiative recombination is not associated with edge effects arising from the cutting of the solar cells only. This chapter was written on the basis of published works. But it should be noted that very

important information relating to this chapter is contained in the article [38], which is being prepared for publication in 2014. It was shown in [38] that at sufficiently high concentrations of free electrons and holes the impact ionization of excitons dominates over their thermal ionization. At such concentrations and the high level of injection the effect causes practically linear sites of dependences the concentration of excitons on the concentration of free charge carriers and of dependences the near-band-edge luminescence intensity in c-Si on the intensity of its excitation.

The work has been partly technically maintained by the Ministry of Education and Sciences of the Russian Federation (State contract 16.526.12.6017). This work was written only thanks to the help to the author in the vital situation, which gave him M.A. Green, E.S. Nevirovich, E.V. Ershov, M.S. Moso'yan, A.A. Mar'in. The author expresses them sincere gratitude.

References

1. Ttupke, T., Zhao, J., Wong, A., Corkish, R., Green, M.A.: Very efficient light emission from bulk crystalline silicon. Appl. Phys. Lett. **82**, 2996–2998 (2003)
2. Green, M.A., Zhao, J., Wang, A., Reece, P.J., Gal, M.: Efficient silicon light-emitting diodes. Nature **412**, 805–808 (2001)
3. Trupke, T., Bardos, R.A., Schibert, M.C., Warta, W.: Photoluminescence imaging of silicon wafers. Appl. Phys. Lett. **89**, 044107-1–044107-3 (2006)
4. Bardos, R.A., Trupke, T., Schubert, M.C., Roth, T.: Trapping artifacts in quasi-steady photoluminescence and photoconductance lifetime measurements on silicon wafers. Appl. Phys. Lett. **88**, 053504-1–053504-3 (2006)
5. Fuyuki, T., Kondo, H., Kaji, Y., Ogane, A., Takahashi, Y.: Analytic findings in the electroluminescence characterization of crystalline silicon solar cells. J. Appl. Phys. **101**, 023711-1–023711-5 (2007)
6. Abbott, M.D., Cotter, J.E., Chen, F.W., Trupke, T., Bardos, R.A., Fisher, K.C.: Application of photoluminescence characterization to the development and manufacturing of high-efficiency silicon solar cells. J. Appl. Phys. **100**, 114514-1–114514-10 (2006)
7. Killani, D., Micard, G., Raabe, B., Herguth, A., Hahn, G.: Minority charge carrier lifetime mapping of crystalline silicon wafers by time-resolved photoluminescence imaging. J. Appl. Phys. **110**, 054508-1–054508-7 (2011)
8. Gundel, P., Heinz, F., Schubert, M.C., Giesecke, J.A., Warta, W.: Quantitative carrier lifetime measurement with micron resolution. J. Appl. Phys. **108**, 033705-1–033705-7 (2010)
9. Mitchell, B., Trupke, T., Weber, J.W., Nyhus, J.: Bulk minority carrier lifetimes and doping of silicon bricks from photoluminescence intensity ratios. J. Appl. Phys. **109**, 083111-1–083111-12 (2011)
10. Green, M.A.: Analytical expressions for spectral composition of band photoluminescence from silicon wafers and bricks. Appl. Phys. Lett. **99**, 131112-1–131112-3 (2011)
11. Mitchell, B., Weber, J.W., Walter, D., Macdonald, D., Trupke, T.: On the method of photoluminescence spectral intensity ratio imaging of silicon bricks: advances and limitations. J. Appl. Phys. **112**, 063116-1–063116-13 (2012)
12. Nærland, T.U., Andelskår, H., Kirkengen, M., Søndenå, R., Marstein, E.S.: The role of excess minority carriers in light induced degradation examined by photoluminescence imaging. J. Appl. Phys. **112**, 033703-1–033703-8 (2012)

13. Altermatt, P.P., Geelhaar, F., Trupke, T., Dai, X., Neisser, A., Daub, E.: Injection dependence of spontaneous radiative recombination in crystalline silicon: experimental verification and theoretical analysis. Appl. Phys. Lett. **88**, 261901-1–261901-3 (2006)
14. Kane, D.E., Swanson, R.M.: The effect of excitons on apparent band gap narrowing and transport in semiconductors. J. Appl. Phys. **73**, 1193–1197 (1993)
15. Emel'yanov, A.M.: The mechanism of radiative recombination in the region of interband transitions in single crystal silicon. Tech. Phys. Lett. **30**(11), 964–966 (2004) (Original Russian text published in Pis'ma Zh. Tekh. Fiz. **30**(22), 75–81 (2004))
16. Emel'yanov, A.M.: Determination of bandgap variations in nondirect-band semiconductors from their edge luminescence spectra. Tech. Phys. Lett. **35**(3), 253–255 (2009) (Original Russian text published in Pis'ma Zh. Tekh. Fiz. **35**(6), 9–16 (2009))
17. Emel'yanov, A.M.: Differential method of analysis of luminescence spectra of semiconductors. Semiconductors **44**, 1134–1139 (2010) (Original Russian text published in Fiz. Tekh. Poluprovodn. **44**, 1170–1175 (2011))
18. Emel'yanov, A.M., Sobolev, N.A.: Silicon light-emitting diodes with strong near-band-edge luminescence. Semiconductors **42**, 329–333 (2008) (Original Russian text published in Fiz. Tekh. Poluprovodn. **42**, 336–340 (2008))
19. Emel'yanov, A.M., Sobolev, N.A.: High-power silicon LEDs with near-band-edge luminescence. Tech. Phys. Lett. **34**(2), 166–168 (2008) (Original Russian text published in Pis'ma Zh. Tekh. Fiz. **34**(4), 64–70 (2008))
20. Emel'yanov, A.M.: Edge photoluminescence of single-crystal silicon with a p–n junction: structures produced by high-efficiency solar cell technology. Semiconductors **45**, 805–810 (2011) (Original Russian text published in Fiz. Tekh. Poluprovodn. **45**, 823–828 (2011))
21. Emel'yanov, A.M.: Edge electroluminescence of heavily doped by boron p^+-n silicon diodes with small area: analysis of modeling representations. Semiconductors **47**, 110–115 (2013) (Original Russian text will be published in Fiz. Tekh. Poluprovodn. **47**, 112–117 (2013))
22. Emel'yanov, A.M.: Edge electroluminescence of single-crystal silicon at 80 K: structures based on high-efficiency solar cell. Phys. Solid State **51**, 244–249 (2009) (Original Russian text will be published in Fiz. Tverd. Tela **51**, 231–236 (2009)
23. Bludau, W., Onton, A., Heinke, W.: Temperature dependence of the band gap of silicon. J. Appl. Phys. **45**, 1846–1848 (1974)
24. Emel'yanov, A.M., Sobolev, N.A., Mel'nikova, T.M., Abrosimov, N.V.: Mechanism of radiative recombination in the region of interband transitions in Si-Ge solid solutions. Fiz. Tekh. Poluprovodn **39**, 1170–1172 (2005). Semiconductors **39**, 1128–1130 (2005)
25. Emel'yanov, A.M., Sobolev, N.A., Mel'nikova, T.M., Abrosimov, N.V.: SiGe light-emitting diodes and their characteristics in the region of band-to-band transitions. Solid State Phenom. **108–109**, 761–766 (2005)
26. Sobolev, N.A., Emel'yanov, A.N., Shek, E.I., Abrosimov, N.V., Yakimenko, A.N.: Efficient SiGe LED on wavelength ~1.3 μm, made by ion implantation. In Proceedings of the 16th International Workshop on Radiation Physics of Solid State, Sevastopol, 3–8 July, 2006, pp. 490–496.
27. Bachrach, R.Z., Lorimor, O.G.: Recombination processes responsible for the room-temperature near-band-gap radiation from GaP. Phys. Rev. B **7**, 700–712 (1973)
28. Altaiskii, Y.M., Avramenko, S.F., Guseva, O.A., Kiselev, V.S.: Electroluminescence of p–n junctions in cubic silicon carbide. Fiz. Tekh. Poluprovodn. **13**, 1978–1983 (1979) [Sov. Phys. Semicond. **13**, 1152–1157 (1979)]
29. Blinov, L.M., Bobrov, E., Vavilov, V.S., Galkin, G.N.: On the recombination of nonequilibrium carriers in silicon at high photoexcitation. Sov. Phys. Solid State **9**, 2537–2541 (1967)
30. Nosov, Y.R.: Physical Principles of Semiconductor Diode Operation in Pulse Regimes. Nauka, Moscow (1968) [in Russian]
31. Ryabtsev, N.G.: Materials for Quantum Electronics. Sovetskoe Radio, Moscow (1972) [in Russian]
32. Emel'yanov, A.M., Sobolev, N.A., Shek, E.I.: Silicon LEDs emitting in the band-to-band transition region: effect of temperature and current strength. Fiz. Tverd. Tela **46**, 44–48 (2004) [Phys. Solid State. **46**, 40–44 (2004)]

33. Emel'yanov, A.M., Nikolaev, Y.A., Sobolev, N.A., Mel'nikova, T.M.: Kinetics of electroluminescence in an efficient silicon light-emitting diode with thermally stable spectral characteristics. Fiz. Tekh. Poluprovodn. **38**, 634–638 (2004) [Semiconductors. **38**, 610–614 (2004)]
34. Emel'yanov, A.M.: Edge luminescence of single-crystal silicon modulated by voltage variation on the p–n junction. Pis'ma Zh. Tekh. Fiz. **35**(18), 80–86 (2009) [Tech. Phys. Lett. **35**, 873–875 (2009)]
35. Michaelis, W., Pilkuhn, M.H.: Radiative recombination in silicon p–n junction. Phys. Stat. Sol. **36**, 311–319 (1969)
36. Nolle, E.L.: Kinetics of recombination via exciton states in semiconductors. Fiz. Tekh. Poluprovodn. **2**, 1679–1682 (1968) [Sov. Phys. Semicond. **2**, 1397–1399 (1968)]
37. Zhao, J., Wang, A., Trupke, T., Green, M.A.: High efficiency bulk crystalline silicon light emitting diodes. Mat. Res. Soc. Symp. Proc. **744**, M4.7.1 (2003)
38. Emel'yanov, A.M.: Impact ionization of excitons in single-crystal silicon and its influence on concentration of excitons and luminescence in the field of fundamental absorption edge. Fiz. Tekh. Poluprovodn. **48**(2), (2014) (in press). Semiconductors **48**(2), (2014) (in press)

.

http://www.springer.com/978-3-319-01987-1

High-Efficiency Solar Cells
Physics, Materials, and Devices
Wang, X.; Wang, Z.M. (Eds.)
2014, XV, 656 p. 367 illus., 256 illus. in color.,
Hardcover
ISBN: 978-3-319-01987-1